Introduction

Intensity-modulated proton therapy (IMPT) has shown the potential to reduce the dose to the organs at risk (OAR), while keeping a similar target coverage compared to intensity-modulated radiation therapy (IMRT) [1, 2] and volumetric modulated arc therapy (VMAT) [2, 3] in head and neck cancer (HNC). Lower dose levels in critical OAR translates into reduced radio-induced toxicities such as xerostomia, dysphagia, or tube feeding dependence [4–8]. However, IMPT is highly sensitive to patient anatomical changes due to the nature of proton interaction with tissues. The initially planned Bragg Peak positions can be altered by density changes along the beam path caused by tumor shrinkage, weight loss, positioning errors or shifts in tumor and organ locations. Fraction after fraction, these uncertainties can cause distortions on the approved clinical plan and compromise plan quality [9–11].

Different techniques have been proposed to mitigate the distortion of the initial plans due to inter-fractional density changes and anatomical deformations: robust treatment planning, offline and online adaptive IMPT. Robust optimization (RO) strategies consider uncertainties during spot weight optimization and lead to dose distributions that are resilient to specific uncertainties, classically systematic setup and range errors [12]. More sophisticated approaches, such as anatomical RO, also include anatomical scenarios during plan optimization [13–15]. Nevertheless, it remains difficult not to compromise the optimality of the IMPT plan while trying to cover a wide range of possible anatomical changes. RO can provide robustness against some density and anatomical changes but it is not the ultimate solution, treatment plan adaptation is still required [3, 11, 16, 17].

A typical full offline adaptation can take several days in the clinical workflow since it requires re-contouring, re-planning, treatment plan approval and additional quality assurance. In the meanwhile new anatomical changes could occur. In order not to delay treatment delivery, another possibility is to perform an online plan adaptation while the patient is on the treatment couch. Implementation of full online adaptation is very challenging since it requires to complete the adaptation workflow steps in a very short time. Ideally, re-contouring would rely on automatic contour propagation based on artificial intelligence tools and/or deformable image registrations but for the moment they cannot be used independently without human intervention [18], and would therefore still require approval by the doctor.

As an alternative, online adaptive strategies based on the restoration of the dose have been proposed [19, 20]. The idea is to keep the planned dose distribution stable in every fraction by generating a new (restored) plan with updated proton beam energies and spot weights. The advantage of these strategies is that they do not require new contour delineation prior to re-optimization, instead planning contours rigidly mapped are used. Promising results illustrate the potential to

mitigate inter-fractional dose distortions while maintaining target coverage for lung [21] and prostate cancer [22].

This study compares a notadapted robust planning strategy (RO) with two active adaptive IMPT strategies: a fully-offline adaptive (FOA) strategy and a robust automatized online adaptive strategy based on dose restoration (DR). The added clinical value and/or limitations of dose restoration in HNC patients with respect to a full adaptive workflow, including the impact of changes in relative positions and shapes of anatomical structures, are investigated.

Material and methods

Patient data and dose prescription

This study included data of ten HNC patients (see Table1), with a planning CT scan (pCT) and four to six repeated CT scans (rCTs) per patient. Clinical treatment plans were generated at the Department of Radiation Oncology of Maastricht University Medical Center (MAASTRO Clinic, Maastricht, The Netherlands) and delivered using the MEVION S250i Proton Therapy System with HYPERSCAN Pencil Beam Scanning [23]. Institutional review board approval was granted for this study. The patients were treated with a prescription dose of 70 GyRBE to the high-dose clinical target volume (CTV) and 54.25 GyRBE to the low-dose CTV in 35 fractions, using a constant relative biological effectiveness (RBE) factor of 1.1. The spinal cord, parotids, submandibulars and the oral cavity were defined as organs at risk (OARs). Target and OAR delineations performed by experienced radiotherapy oncologists were available in all pCTs and rCTs.

Treatment planning and adaptation strategies

Three different planning strategies aiming at clinically acceptable doses in each rCT were compared. Robust optimization (RO) planning without treatment adaptation and two active adaptation strategies: online dose restoration (DR) and full offline adaptation (FOA), were applied and evaluated as described in Fig 1. All dose calculations were run in RayStation 10A (Raysearch Laboratories, Stockholm, Sweden) using the Monte Carlo algorithm in a 3.0 × 3.0 × 3.0 mm^3 dose grid.

(1) Robust optimization (RO)

A robustly optimized treatment plan was created on the pCT applying classical worst-case robust optimization (setup error (SE) = 3 mm, range error (RE) = 3%). SE scenarios included patient shifts in the three axes of the space x,y,z (±SE, 0, 0), (0, ±SE, 0), (0, 0, ±SE) and the nominal scenario (0,0,0). Range robustness was also included to account for uncertainties in the conversion from CT numbers to proton stopping power ratios. RE scenarios were modeled by scaling the mass density by

±3%. The nominal scenario (i.e. 0%) was also included. The combination of seven SE scenarios and three RE scenarios lead to an optimization with twenty-one (7x3) error scenarios.

(2) Dose Restoration (DR)

The dose restoration approach used in this study was the isodose volume dose restoration, an in-house developed workflow introduced by Bernatowicz et al [19] and further investigated by Borderias et al [21]. Dose restoration was fully-automatized using RayStation scripting but required the additional generation of a pre-treatment plan compared to a regular planning procedure (see Fig 1).

First, isodose contours were constructed from the clinical dose in the original plan on the pCT (every 2 Gy within 95%–107% of the prescription dose and 5 Gy outside). Later, still at the planning stage, optimization parameters (i.e a set of weighted minimum and maximum objectives) were manually tuned in order to generate the so-called isodose-based optimized (IBO) plan, which reproduces the planned isodose distributions. Robust objectives were set for the isodoses corresponding to prescription dose levels (70 and 54.25 Gy) and the CTVs. The isodose levels and optimization parameters of the IBO plan were saved in a patient-specific template (IBO template) to be further used for fully-automatized dose restoration on rCT as follows.

After the acquisition of the rCT, automatic rigid registration based on the bony anatomy was performed between the pCT and the rCTs. Then, the previously generated isodose contours and delineated CTVs and OAR on the pCT were rigidly mapped to the rCT. The clinical plan on the pCT was used as a warm-start for adaptation. The same beam configuration, beam computation settings, robustness parameters and spot position initialization were used for re-optimization together with the patient-specific IBO template generated on the pCT. Restored plans were characterized by updated spot weights.

(3) Full offline adaptation (FOA)

Instead of using rigidly mapped contours, FOA plans were manually and robustly re-optimized based on manually delineated contours available on the rCTs. The same optimization objectives as in the clinical plans on the pCT were used. Objective weights were manually adjusted to meet the clinical goals and extra optimization objectives were added if necessary.

Robust evaluation of the strategies

The clinical plan robustly optimized on the pCT, the DR plan and the FOA plan were robustly evaluated on the rCTs with the same strategy. Robust evaluation was

performed simulating 28 uncertainty scenarios (14 SE scenarios x 2 RE scenarios) for each of the plans. As described in Fig 1.b, the sampling of the setup error scenarios included the 6 principal directions (6 red dots) and the diagonals from the center to the vertices (8 green dots) as suggested in Korevaar et al [24]. Nominal and worst-case values out of all scenarios were reported for each metric on the manually delineated contours, i.e. maximum values for OAR metrics and minimum values for CTV coverage.

From this point on, we will refer to the evaluation (i.e. re-calculation) of the clinical plan on rCTs as the non-adapted (NA) plan, as this plan was not actively adapted. Plan parameters such as energy layers, number of spots or spot weights were not modified when recomputing the dose for this plan on the rCTs.

Comparison metrics

The following dose volume parameters were evaluated for both the high- and low-dose target volumes: D98% ≥ 95% and D2% ≤ 107% of the prescription dose, where D98% and D2% are the doses received at 98% and 2% of the target volume, respectively. For the OARs, the constraints were: $D0.03cm^3$ < 45 Gy in the spinal cord, Dmean < 26 Gy to both parotids, both submandibular glands and the oral cavity. Nominal (SE = 0 mm, RE = 0%) and worst-case values were reported from the robustness evaluations of NA, DR and FOA plans. Median values and interquartile range (IQR) were calculated for each metric over the 50 rCTs.

Wilcoxon signed-rank tests were performed to assess the statistical significance of the differences between dose metrics for each strategy. We were interested in the performance of adaptation workflows (DR and FOA), especially when not-adapted plans were distorted (i.e., not meeting the clinical goals on the rCTs). Hence, for cases where the not-adapted plan differed less than 0.5 Gy with respect to the clinical plan on the pCT were not included in the significance tests. A p-value < 0.05 was considered statistically significant.

The DICE similarity coefficient was calculated between the manually delineated and rigidly mapped contours on the rCTs to quantify the accuracy of the rigid registration between the pCT and the rCTs.

Results

For the NA plans, the clinical goals for the target coverage (i.e., D98% ≥ 95%) in the nominal scenario were only met in 26% (13/50) of the rCTs. After performing DR, the percentage was increased to 52% (26/50). All plans met all clinical goals when full off-line adaptation was applied.

Fig 2. shows the differences in DVH-metrics between the approved clinical plan on the pCT and the NA, DR, and FOA plans in the OAR and CTVs with two prescription levels: high-dose CTV and low-dose CTV. Target coverage (D98%) of the high-dose CTV was significantly lower for NA plans compared to the DR and FOA plans (both $p<0.0001$), with median values of the difference with respect to the clinical plan of -0.8 (IQR=1.3) Gy, -0.1 (IQR=1.0) Gy and -0.1 (IQR=0.2) Gy, respectively.

The over-dosage of the high-dose CTV, characterized by D2%, showed a similar trend, with median values of the difference with respect to the clinical plan of 0.53 (IQR=1.34) Gy, 0.19 (IQR=0.56) Gy and 0.03 (IQR=0.36) Gy for the NA, DR and FOA plans, respectively. Once again, differences between DR and FOA with respect to NA were significant (both $p<0.0001$).

Target coverage (D98%) of the low-dose CTV was lower than for the clinical plan for both NA and DR plans with the same median values but with a lower variability for the DR plans: differences of -0.7 (IQR=2.3) Gy for NA and -0.7 (IQR=1.2) Gy for DR. Analyzing only distortions greater than 0.5 Gy in NA plans, significant differences were found for DR plans compared to NA plans in nominal scenarios ($p = 2.1\cdot 10^{-4}$). Differences in the worst-case D98% values between NA and DR were also significant for both CTVs ($p = 7.8\cdot 10^{-4}$ and $p = 3.8\cdot 10^{-4}$ for low-risk and high-risk CTVs, respectively).

Regarding critical OAR, such as the spinal cord, the DR plans offered a significant sparing, in comparison to the NA plans, for both the nominal scenario and worst-case scenario. Dose differences in the right submandibular gland and the oral cavity were not significant between the three methods in nominal or worst-case values.

Fig 3. illustrates three patient examples where DR corrected the distortions in NA plans. Patient 3, who experienced a reduction of the lateral neck diameter, and patient 8, with a suboptimal re-positioning of the shoulders, presented significant under-dosages for the low-dose and high-dose CTV in the NA plan, respectively. DR was able to recover isodose 95% of the prescribed doses in both cases, improving dose conformality and robustness.

However, outliers, showing critical under-dosage in CTVs(D98%) or over-dosage for the spinal cord $D0.03cm^3$, highlighted the limitations of DR to improve plan quality in some cases. Dose distributions associated with two of these patients are shown in Fig 4. For patient 1, cold spots were visible in the low-dose CTV of both the NA and DR plans in the second rCT. In this case, DR did reproduce the dose distribution on the rCT, but not at the correct location since the rigid registration between pCT and rCT could not compensate for the non-rigid deformations on the lower part of low-dose CTV due to an inaccurate shoulder repositioning (see supplementary

material). This led to a sub-optimal overlap between the delineated and rigidly mapped low-dose CTV characterized by a DICE coefficient of 0.78. As shown for patient 2 (Fig 4.b), anatomical deformations involving relative movement between targets and OAR are also a cause of poor alignment between manual and rigidly mapped contours. High-dose CTV shrinkage of 11.5% together with a shift in the cranio-caudal direction and a more pronounced neck curvature in the rCT led to the spinal cord moving into the dose distribution (the DICE score between the manually delineated and the rigidly mapped spinal cord contour was 0.56 for this rCT). Furthermore, some part of the high-dose CTV moved slightly outside the high-dose region (the DICE score for the high-dose CTV was 0.74). For both these patients, a full offline adaptation was required to achieve an optimal target coverage.

Discussion

Two adaptive strategies (1) online dose restoration and (2) full offline adaptation were compared in this study against not-adapted robustly optimized plans. Both strategies used robust optimization and aimed at mitigating dose distortions of IMPT plans induced by inter-fractional anatomical changes in a set of 50 rCTs for ten HNC patients.

It was shown that online dose restoration had the potential to reduce the need for offline adaptation of robustly optimized plans from 74% (37/50) to 48% (24/50). Three main findings can be extracted from our results.

First, robust optimization with the used parameters did not ensure adequate robustness levels against most anatomical changes observed in this study making the implementation of adaptive strategies indispensable. However, although many centers wish to implement adaptation workflows, they face barriers of human/material resources and technical limitations [25]. Dose restoration can be easily implemented for any tumor location and planning strategy. 4D-robust dose restoration was tested in lung cancer patients with a PROTEUS1 (IBA, Belgium) beam model [21] and thanks to the flexibility of the scripting module of RayStation, the workflow was adapted without difficulty to HNC patients treated with a MEVION beam model. Moreover, the simplicity of dose restoration allows its implementation in other treatment planning systems. Therefore, we believe dose restoration is accessible to any group interested in adaptive IMPT.

Second, as it has already been shown for other locations, such as lung tumors by Borderias et al. [21] or prostate by Jagt et al. [22], online dose restoration strategies using spot intensity re-optimization have the potential to automatically and successfully restore the clinical plan on rCTs. Hence, the clinical implementation of dose restoration could ensure target coverage for patients where robust treatment plans tend to be distorted. This result agrees with the results found by van de Water et al. [18], where superior target coverage and OAR sparing were shown for daily

online dose restoration compared to robust optimization approaches in cases with artificially generated cavity filling.

Third, our study highlighted the intrinsic limitations of dose restoration which are especially remarkable in HNC. For a specific subset of patients, both robust and restored plans could not compensate for large anatomical changes which compromised the target coverage, making a cumbersome full offline re-planning still mandatory. Challenging shoulder repositioning seems to be especially critical for low-dose CTV coverage [26, 27] while the reduction of the neck diameter or drastic non-rigid deformations can affect both low and high-dose CTVs. Lalonde et al. [28] proposed an alternative online adaptation strategy using non-rigidly deformed contours which showed a higher efficiency with respect to classical and anatomical robust optimization. However, the use of this technique comes at the cost of the need for contour verification and doctor approval.

The selection of patients who would benefit from dose restoration is crucial since highly sensitive action levels towards offline adaptation may result in frequent adaptation with little clinical gain at the cost of a high stress on human resources. Our study suggests potential DICE thresholds that could be defined for patient selection. It was found that low DICE coefficients (<0.75) between rigidly mapped and manually delineated contours seemed to properly trigger cases where DR could not ensure sufficient target coverage. On the contrary, for high DICE coefficients (>0.90) all restored plans had optimal target coverage (see Supplementary material). However, further investigation is needed in a larger cohort of patients to assess the usability of DICE coefficient as a trigger for the use of DR. For intermediate cases ($0.75 < DICE < 0.90$), a fast-independent dose calculation could also help to select the appropriate adaptation strategy and as a pre-treatment patient-specific QA procedure. Since the manually delineated contours are not available immediately after a rCT is acquired, deformable image registration or automatic segmentations tools [29] could be used in this evaluation step. Other parameters such as the degree of weight loss and reduction in lateral neck diameter could also be monitored as predictors of patients receiving the greatest benefit of adaptation [30]. In any case, all online adapted plans should be followed by a more extensive QA analysis including machine log files after delivery [31].

As previously mentioned, the two key points of dose restoration are (1) no need for manual re-contouring and (2) maintenance of unchanged dose distribution on rCTs to minimize or even by-pass the physician’s approval step. However, we have seen that there are limitations to this approach. Emerging commercial solutions for conventional radiation therapy using CBCT based workflows can already create plans with completely new dose distributions adapted to a new anatomy in a few minutes [32]. Similarly, an ideal IMPT adaptive workflow could use, for example, deep learning models for automatic contour segmentation [33, 34] followed by dose prediction [35, 36] and a dose mimicking optimization algorithm [37, 38]. However,

quality assurance processes required to verify completely new plan designs may make online adaptation cumbersome for clinical implementation.

In our study, the total time for plan adaptation ranged between 11.9 and 23.1 min, with a median of 17.4 min. The median time distribution was 6.2 min for the first step including pCT-rCT rigid registration, contour mapping and loading spot information and 11.2 min for spot intensity robust re-optimization. This time could be different for other treatment machines than the proton therapy and dose calculation algorithm used in our study (MEVION S250i) which requires the computation of accurate dose scenarios during Monte Carlo optimization in the planning system due to the use of the multi-leaf collimator. Using interpolation during optimization in RayStation can reduce the optimization time by a factor of three. In any case, the time lost was purely computational, and therefore its reduction should be addressed via hardware investment or the improvement of optimization algorithms.

In conclusion, automatic online dose restoration could reduce the offline adaptation rate in HNC IMPT treatments, saving valuable human and material resources to radiotherapy departments. Unfortunately, full offline adaptation was still necessary for 48% of the cases and only a reduced group of patients suffering specific density changes could benefit from dose restoration.

References

1. van de Water TA, Lomax AJ, Bijl HP, et al (2011) Potential benefits of scanned intensity-modulated proton therapy versus advanced photon therapy with regard to sparing of the salivary glands in oropharyngeal cancer. Int J Radiat Oncol Biol Phys 79:1216–1224

2. Simone CB, Ly D, Dan TD, et al (2011) Comparison of intensity-modulated radiotherapy, adaptive radiotherapy, proton radiotherapy, and adaptive proton radiotherapy for treatment of locally advanced head and neck cancer. Radiother Oncol 101.: https://doi.org/10.1016/j.radonc.2011.05.028

3. Góra J, Kuess P, Stock M, et al (2015) ART for head and neck patients: On the difference between VMAT and IMPT. Acta Oncol 54:1166–1174

4. Meijer TWH, Scandurra D, Langendijk JA (2020) Reduced radiation-induced toxicity by using proton therapy for the treatment of oropharyngeal cancer. Br J Radiol 93:20190955

5. van der Laan HP, van de Water TA, van Herpt HE, et al (2013) The potential of intensity-modulated proton radiotherapy to reduce swallowing dysfunction in the treatment of head and neck cancer: A planning comparative study. Acta Oncol 52:561–569

6. Ahn P, Lin A, Zhou O, et al (2016) A Comparative Study of Patient-Reported Quality of Life, Xerostomia, and Dysgeusia in Oropharyngeal Squamous Cell Carcinoma (OPSCC) Treated With Volumetric Modulated Arc Therapy (VMAT) or Proton Pencil Beam Scanning (PBS). International Journal of Radiation Oncology*Biology*Physics 94:883–884

7. Manzar GS, Lester SC, Routman DM, et al (2020) Comparative analysis of acute toxicities and patient reported outcomes between intensity-modulated proton therapy (IMPT) and volumetric modulated arc therapy (VMAT) for the treatment of oropharyngeal cancer. Radiotherapy and Oncology 147:64–74

8. Chou YC, Hung SP, Hsieh CE, et al (2018) Intensity-Modulated Proton Therapy Reduces Acute Treatment-Related Toxicities for Patients with Nasopharyngeal Cancer: A Case-Control Propensity Score Match Study with Volumetric Modulated Arc Therapy. International Journal of Radiation Oncology*Biology*Physics 102:e236–e237

9. Lomax AJ (2008) Intensity modulated proton therapy and its sensitivity to treatment uncertainties 1: the potential effects of calculational uncertainties. Physics in Medicine and Biology 53:1027–1042

10. Lomax AJ (2008) Intensity modulated proton therapy and its sensitivity to treatment uncertainties 2: the potential effects of inter-fraction and inter-field motions. Physics in Medicine and Biology 53:1043–1056

11. Müller BS, Duma MN, Kampfer S, et al (2015) Impact of interfractional changes in head and neck cancer patients on the delivered dose in intensity modulated radiotherapy with protons and photons. Phys Med 31:266–272

12. Liu W, Frank SJ, Li X, et al (2013) Effectiveness of robust optimization in intensity-modulated proton therapy planning for head and neck cancers. Med Phys 40:051711

13. van de Water S, Albertini F, Weber DC, et al (2018) Anatomical robust optimization to account for nasal cavity filling variation during intensity-modulated proton therapy: a comparison with conventional and adaptive planning strategies. Phys Med Biol 63:025020

14. Cubillos-Mesías M, Troost EGC, Lohaus F, et al (2019) Including anatomical variations in robust optimization for head and neck proton therapy can reduce the need of adaptation. Radiother Oncol 131:127–134

15. Yang Z, Zhang X, Wang X, et al (2020) Multiple-CT optimization: An adaptive optimization method to account for anatomical changes in intensity-modulated proton therapy for head and neck cancers. Radiother Oncol 142:124–132

16. Bobić M, Lalonde A, Sharp GC, et al (2021) Comparison of weekly and daily online adaptation for head and neck intensity-modulated proton therapy. Phys Med Biol. https://doi.org/10.1088/1361-6560/abe050

17. Kraan AC, van de Water S, Teguh DN, et al (2013) Dose uncertainties in IMPT for oropharyngeal cancer in the presence of anatomical, range, and setup errors. Int J Radiat Oncol Biol Phys 87:888–896

18. Lim JY, Leech M (2016) Use of auto-segmentation in the delineation of target volumes and organs at risk in head and neck. Acta Oncol 55:799–806

19. Bernatowicz K, Geets X, Barragan A, et al (2018) Feasibility of online IMPT adaptation using fast, automatic and robust dose restoration. Phys Med Biol 63:085018

20. Jagt T, Breedveld S, van de Water S, et al (2017) Near real-time automated dose restoration in IMPT to compensate for daily tissue density variations in prostate cancer. Phys Med Biol 62:4254–4272

21. Borderías Villarroel E, Geets X, Sterpin E (2020) Online adaptive dose

restoration in intensity modulated proton therapy of lung cancer to account for inter-fractional density changes. Phys Imaging Radiat Oncol 15:30–37

22. Jagt TZ, Breedveld S, van Haveren R, et al (2020) Online-adaptive versus robust IMPT for prostate cancer: How much can we gain? Radiother Oncol 151:228–233

23. Vilches-Freixas G, Unipan M, Rinaldi I, et al (2020) Beam commissioning of the first compact proton therapy system with spot scanning and dynamic field collimation. Br J Radiol 93:20190598

24. Korevaar EW, Habraken SJM, Scandurra D, et al (2019) Practical robustness evaluation in radiotherapy – A photon and proton-proof alternative to PTV-based plan evaluation. Radiotherapy and Oncology 141:267–274

25. Bertholet J, Anastasi G, Noble D, et al (2020) Patterns of practice for adaptive and real-time radiation therapy (POP-ART RT) part II: Offline and online plan adaption for interfractional changes. Radiother Oncol 153:88–96

26. Neubauer E, Dong L, Followill DS, et al (2012) Assessment of shoulder position variation and its impact on IMRT and VMAT doses for head and neck cancer. Radiat Oncol 7:19

27. Tachibana H, Motegi K, Moriya S (2018) Impact of shoulder deformation on volumetric modulated arc therapy doses for head and neck cancer. Physica Medica 53:118–128

28. Lalonde A, Bobić M, Winey B, et al (2021) Anatomic changes in head and neck intensity-modulated proton therapy: Comparison between robust optimization and online adaptation. Radiother Oncol 159:39–47

29. Kosmin M, Ledsam J, Romera-Paredes B, et al (2019) Rapid advances in auto-segmentation of organs at risk and target volumes in head and neck cancer. Radiother Oncol 135:130–140

30. Capelle L, Mackenzie M, Field C, et al (2012) Adaptive radiotherapy using helical tomotherapy for head and neck cancer in definitive and postoperative settings: initial results. Clin Oncol 24:208–215

31. Li H, Sahoo N, Poenisch F, et al (2013) Use of treatment log files in spot scanning proton therapy as part of patient-specific quality assurance. Medical Physics 40:021703

32. Sibolt P, Andersson LM, Calmels L, et al (2021) Clinical implementation of artificial intelligence-driven cone-beam computed tomography-guided

online adaptive radiotherapy in the pelvic region. Phys Imaging Radiat Oncol 17:1–7

33. Cardenas CE, Beadle BM, Garden AS, et al (2021) Generating High-Quality Lymph Node Clinical Target Volumes for Head and Neck Cancer Radiation Therapy Using a Fully Automated Deep Learning-Based Approach. Int J Radiat Oncol Biol Phys 109:801–812

34. Wong J, Fong A, McVicar N, et al (2020) Comparing deep learning-based auto-segmentation of organs at risk and clinical target volumes to expert inter-observer variability in radiotherapy planning. Radiother Oncol 144:152–158

35. Guerreiro F, Seravalli E, Janssens GO, et al (2021) Deep learning prediction of proton and photon dose distributions for paediatric abdominal tumours. Radiother Oncol 156:36–42

36. Barragán-Montero AM, Nguyen D, Lu W, et al (2019) Three-dimensional dose prediction for lung IMRT patients with deep neural networks: robust learning from heterogeneous beam configurations. Medical Physics 46:3679–3691

37. McIntosh C, Welch M, McNiven A, et al (2017) Fully automated treatment planning for head and neck radiotherapy using a voxel-based dose prediction and dose mimicking method. Phys Med Biol 62:5926–5944

38. Petersson K, Nilsson P, Engström P, et al (2016) Evaluation of dual-arc VMAT radiotherapy treatment plans automatically generated via dose mimicking. Acta Oncol 55:523–525

Tables

Patient	Adaptation	Location	N_beams	Days after pCT for each rCT					
				1rCT	2rCT	3rCT	4rCT	5rCT	6rCT
1	Y	Nasopharynx	7	20	27	34	41	48	55
2	Y	Larynx	4	25	33	39	47	-	-
3	Y	Oropharynx	5	17	23	30	36	44	-
4	N*	Oropharynx	5	16	23	30	37	44	-
5	Y	Oropharynx	5	15	22	28	35	41	44
6	Y	Oropharynx	4	24	29	38	44	50	-
7	Y	Hypopharynx	4	26	34	40	43	-	-
8	N*	Nasopharynx	9	21	28	35	42	49	-
9	Y	Hypopharynx	5	18	22	29	36	43	54
10	Y	Oropharynx	5	10	17	24	31	-	-

Table 1. Characteristics of the head and neck IMPT patient data-base. *Abbreviations: Y = Yes, N = No, pCT = planning-CT, rCT=repeated-CT, *Patients not being adapted during treatment but with clinical goals not achieved in some of the fractions.*

Figures

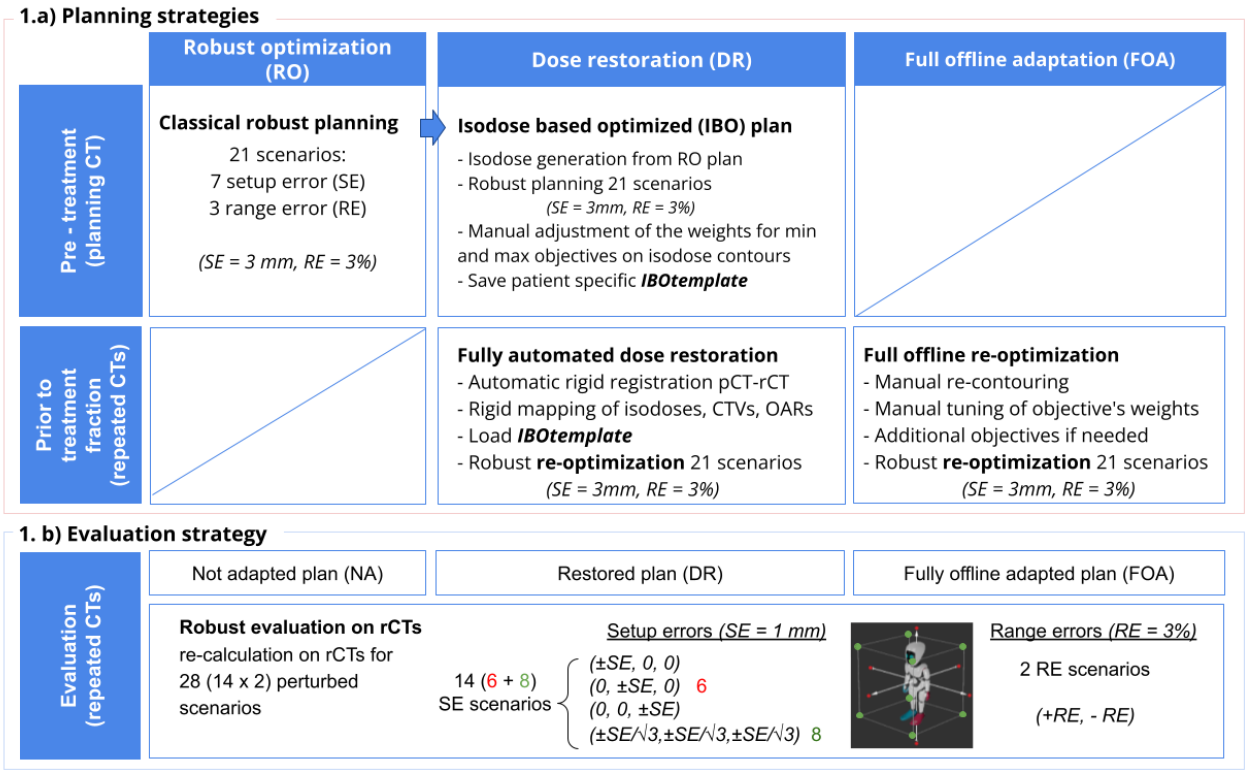

Fig 1. Summary of a) the three planning strategies compared in this study and b) the robustness evaluation.

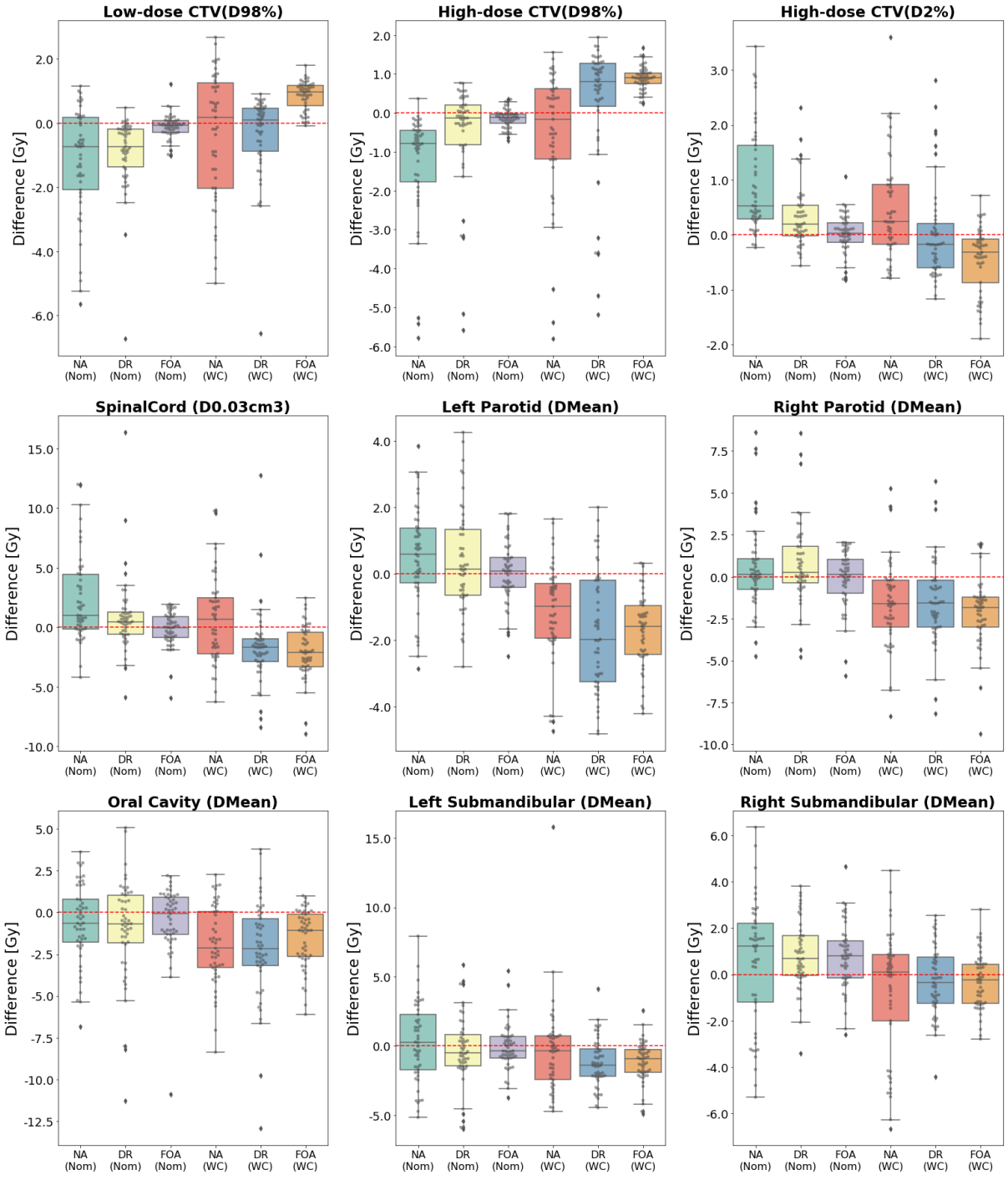

Fig 2. Differences in DVH-metrics with respect to clinical plan on the planningCT for not-adapted (NA), restored (DR) and fully offline adapted (FOA) plans for the nominal dose distribution (green, yellow and purple) and worst-case values (red, blue and orange) were reported for 50 rCTs. *Abbreviations: D98% = dose received by 98% of the volume, D2% = dose received by 2% of the volume, Dmean = mean dose, D0.03cm^3 = dose received by a volume of 0.03 cm^3, Nom = nominal, WC = worst-case.*

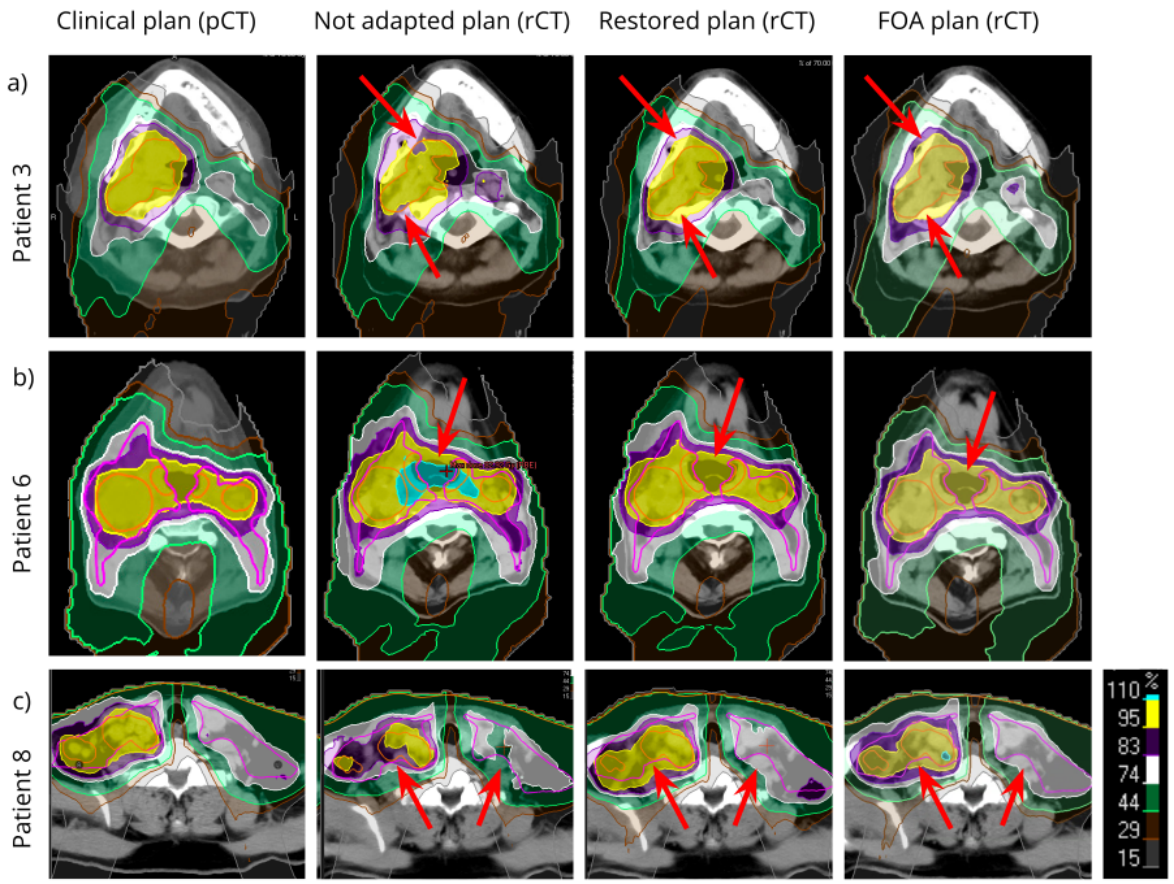

Fig 3. Nominal dose distributions in three representative patients for which DR ensured target coverage but NA did not.. Red arrows highlight regions of over- or under-dosage. Isodoses are represented with different colors as a percentage of the prescribed dose, the yellow isodose is 95%(70 Gy) and the white isodose is 95%(54.25Gy).

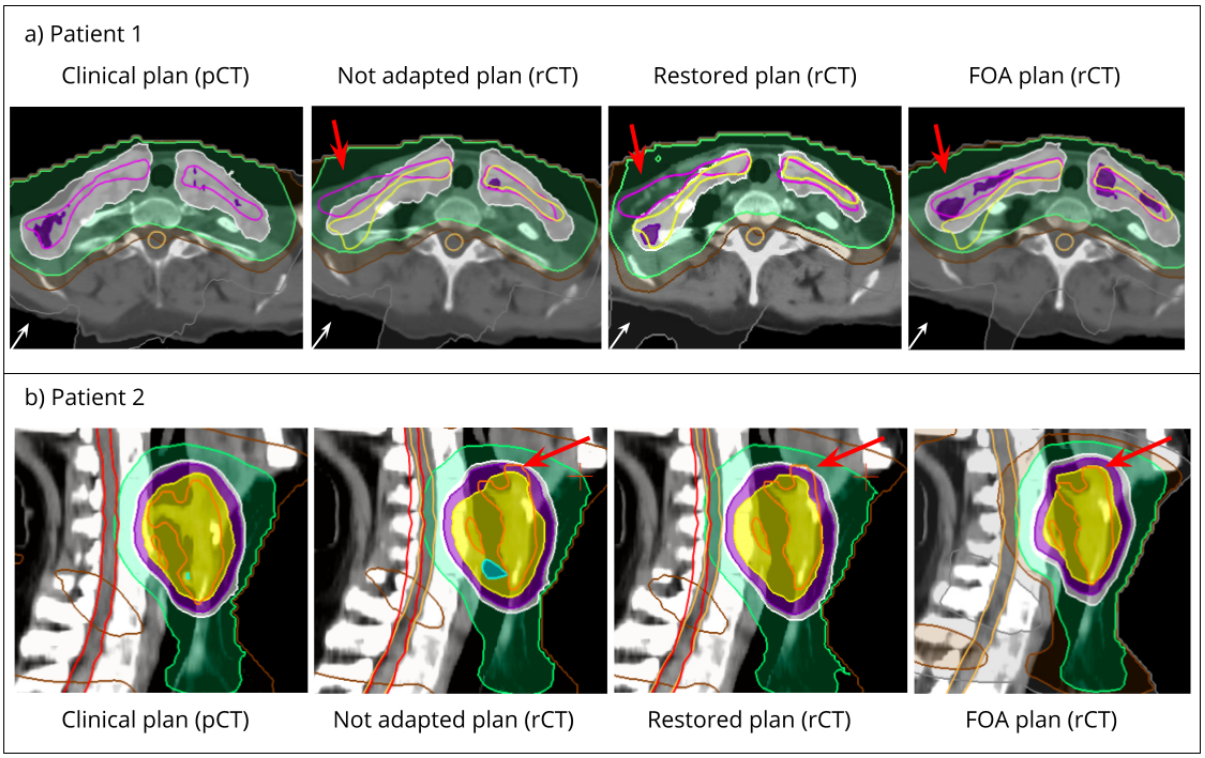

Fig 4. Nominal dose distributions in two representative patients where DR was not sufficient to ensure full target coverage. Red arrows highlight regions of over- or under-dosage. Isodoses are represented with different colors as a percentage of the prescribed dose, the yellow isodose is 95%(70 Gy) and the white isodose is 95%(54.25Gy). a) The yellow contour is the rigidly mapped low-dose CTV and the magenta contour is the manually delineated low-dose CTV. b) The orange contour is the manually delineated high-dose CTV.

Captions

Table 1. Characteristics of the head and neck IMPT patient data-base. *Abbreviations: Y = Yes, N = No, pCT = planning-CT, rCT=repeated-CT, *Patients not being adapted during treatment but with clinical goals not achieved in some of the fractions.*

Fig 1. Summary of a) the three planning strategies compared in this study and b) the robustness evaluation.

Fig 2. Differences in DVH-metrics with respect to clinical plan on the planningCT for not-adapted (NA), restored (DR) and fully offline adapted (FOA) plans for the nominal dose distribution (green, yellow and purple) and worst-case values (red, blue and orange) were reported for 50 rCTs. *Abbreviations: D98% = dose received by 98% of the volume, D2% = dose received by 2% of the volume, Dmean = mean dose, D0.03cm^3 = dose received by a volume of 0.03 cm^3, Nom = nominal, WC = worst-case.*

Fig 3. Nominal dose distributions in three representative patients for which DR ensured target coverage but NA did not.. Red arrows highlight regions of over- or under-dosage. Isodoses are represented with different colors as a percentage of the prescribed dose, the yellow isodose is 95%(70 Gy) and the white isodose is 95%(54.25Gy).

Fig 4. Nominal dose distributions in two representative patients where DR was not sufficient to ensure full target coverage. Red arrows highlight regions of over- or under-dosage. Isodoses are represented with different colors as a percentage of the prescribed dose, the yellow isodose is 95%(70 Gy) and the white isodose is 95%(54.25Gy). a) The yellow contour is the rigidly mapped low-dose CTV and the magenta contour is the manually delineated low-dose CTV. b) The orange contour is the manually delineated high-dose CTV.